Box-Behnken Optimization of Folic Acid-Functionalized Mesoporous Silica Nanoparticles for Silymarin Delivery in Alcohol-Induced Hepatocellular Carcinoma

Nithyananth[1*], Akilan[2]

[1], [2] Department of pharmaceutics, PSG College of Pharmacy, Coimbatore, Tamil Nadu, India, Affiliated to The Tamil Nadu Dr. M. G. R Medical University, Chennai.

*Corresponding author:

Mr. M. Nithyananth, M. Pharm.,

Department of Pharmaceutics,

PSG College of Pharmacy, Coimbatore, Tamil Nadu, India.

Affiliated to The Tamil Nadu Dr. M. G. R Medical University, Chennai, India.

ABSTRACT

Background: Silymarin (SL) a natural flavonolignan, exhibits notable hepatoprotective and anticancer properties. However, its clinical application is hindered by poor aqueous solubility and low bioavailability, limiting therapeutic efficacy in liver cancer treatment. To overcome these drawbacks, this study developed and evaluated silymarin-loaded folic acid-coated mesoporous silica nanoparticles (FA-MSNs) as a novel targeted drug delivery system.

Results: The optimized SL-FA-MSNs demonstrated a uniform particle size of 653.9 nm, a polydispersity index (PDI) of 0.2, and a zeta potential of −13.4 mV, indicating high stability and minimal aggregation. Successful drug encapsulation was confirmed through Fourier transform infrared spectroscopy (FTIR), scanning electron microscopy (SEM), X-ray diffraction (XRD), and atomic force microscopy (AFM) analyses. In vitro release studies revealed a significantly enhanced release profile, with FA-MSNs achieving 67.9% drug release over 24 hours compared to 39.4% for free silymarin. Cytotoxicity assays on HepG2 liver cancer cells showed prolonged anticancer activity, with FA-MSNs displaying an IC_{50} value of 55.750 µg/mL, higher than that of free silymarin (39.877 µg/mL), suggesting improved safety and controlled drug release.

Conclusion: FA-MSNs effectively enhanced the solubility, stability, and sustained release of silymarin while enabling targeted delivery to cancer cells. The formulation demonstrated improved therapeutic potential with reduced cytotoxicity toward non-target cells, supporting its role as a promising nanocarrier for liver cancer therapy. These findings suggest that FA-MSN-based drug delivery platforms can minimize systemic side effects, enhance bioavailability, and improve treatment outcomes, providing a viable approach for the clinical translation of silymarin in oncology.

Keywords: Silymarin, FA-MSNs, Liver cancer, Drug delivery, Nanocarrier, Sustained release, Targeted therapy.

1. INTRODUCTION:

Liver cancer is the main cause of cancer-related mortality in the global population, with hepatocellular carcinoma being the most frequent type of cancer [1]. Hepatocellular carcinoma is now the third leading cause of cancer-related death and the sixth most common type of cancer diagnosed globally, is increasingly driven by alcohol-related liver disease; this study applies Box-Behnken optimization to develop folic acid-functionalized mesoporous silica nanoparticles for targeted silymarin delivery to improve outcomes in alcohol-induced Hepatocellular carcinoma [2]. Clinically, alcohol-related Hepatocellular carcinoma (ALD-HCC) presents sicker patients with worse liver function and poorer overall condition than non-alcohol etiologies—making drug delivery and tolerability particularly challenging [3]. Even modest alcohol exposure escalates cirrhosis risk, and cirrhosis is the dominant substrate for Hepatocellular carcinoma HCC; risk persists despite partial abstinence, strengthening the case for adjunct chemoprevention/therapy approaches [4]. Silymarin—an antioxidant/anti-inflammatory flavonolignan mixture—shows hepatoprotective signals in clinical trials (enzyme reductions) and is generally safe even at high doses, but pharmacokinetic limitations blunt efficacy [5]. The core limitation is biopharmaceutics: silymarin has very low aqueous solubility and poor oral bioavailability, prompting formulation strategies to enhance absorption and exposure [6]. Modern formulations improve exposure but still face ceilings; recent nanocrystal and micellar products enhanced silybin/silymarin bioavailability in animals and humans, yet targeted delivery to diseased liver tissue remains an unmet need [7]. Mesoporous silica nanoparticles (MSNs) offer high surface area, tunable pores, and robust cargo capacity with favorable biosafety and degradability profiles—making them strong candidates for difficult, poorly soluble actives like silymarin [8]. For liver diseases, MSNs enable multifunctional design (stimuli-responsive release, imaging, and targeting) and have been specifically explored for hepatic applications, laying the groundwork for a silymarin–MSN platform [9]. Active targeting can further increase the therapeutic index; folic acid (FA) ligands exploit folate receptor (FR) overexpression on malignant cells and tumour microenvironments, improving uptake and cytotoxic delivery in multiple cancer models [10]. Importantly for HCC, recent clinical-translational data report elevated folate receptor 1 (FOLR1) in tumours and serum of HCC patients with diagnostic/prognostic value—supporting FA as a rational targeting handle in liver cancer [11]. Folic Acid FA-modified nanocarriers enhance tumour-cell internalization and potency versus non-targeted systems; studies with FA-decorated particles show improved uptake and apoptosis in cancer cells, a principle extendable to silymarin payloads [12]. Despite many silymarin formulations, few leverage FA-functionalized MSNs specifically for ALD-HCC pathophysiology, where oxidative stress, inflammation, and fibrotic remodeling are prominent and could be addressed by targeted antioxidant delivery [13].

The design-of-experiments (DoE) optimization for MSN formulations that carry phytochemicals is underutilized, particularly regarding comprehensive response-surface approaches such as encapsulation, size, PDI, zeta potential, and release for silymarin–FA-MSNs [14]. Box–Behnken Design (BBD) is a DoE workhorse that efficiently maps factor–response relationships with fewer runs than many alternatives, enabling statistically robust optimization of nanoparticle attributes critical for in vivo performance [15]. Current

nanomedicine and materials studies increasingly employ BBD with Design-Expert® to optimize nano-formulations and delivery systems—validating BBD as a practical, reproducible framework for MSN tuning [16]. Pairing a hepatoprotective yet PK-limited drug (silymarin) with a safe, tunable carrier (MSNs), equipped with a clinically relevant targeting ligand (FA), and statistically optimized via BBD, directly addresses solubility, targeting, and controlled release barriers in ALD-HCC [11]. Integrating FA-MSNs with silymarin for alcohol-induced HCC is timely given new data on alcohol-attributable liver cancer burden and the inferior clinical status of ALD-HCC patients, who may benefit most from targeted, lower-dose regimens [3].

2. MATERIALS AND METHOD:

Silymarin, cetyltrimethylammonium bromide, tetra ethyl ortho silicate, sodium silicate, and silica dioxide were purchased from Otto Chemie, Mumbai. Methanol was obtained from Loba Chemie Pvt. Ltd., Mumbai. Span 80 and Tween 80 were bought from SD Fine Chem, Mumbai.

2.1 Preparation of Screening MSNs and Preparation of Optimization of MSNs:

Screening different silica sources and surfactants is essential to optimize the synthesis of mesoporous silica nanoparticles (MSNs) with desired pore size, morphology, and surface properties. Tetraethyl orthosilicate provides highly uniform and pure silica structures, sodium silicate with rapid hydrolysis, while silica dioxide serves as a direct, preformed silica base. Surfactants such as cetyltrimethylammonium bromide create ordered pore channels, Tween 80 is forming stable emulsions with biocompatible surfaces, and Span 80 supports larger pore formation through hydrophobic interactions. Silica acts as the main structural framework of MSNs, while surfactants guide pore arrangement and size control, making both indispensable for producing nanoparticles with high surface area, tunable porosity, and targeted drug delivery efficiency. Dissolve surfactant in water-ethanol, stir 15 min at 80°C. Add 2 M NaOH and silica source, stir 24 h. Homogenize 10 min at 1000 rpm, then centrifuge at 4000 rpm (40 min × 3). Sonicate 10 min; mesoporous silica is ready for use [17]. Screening is Shown in Table 1. Result shown in Fig 1.

Table 1 Screening MSNs different Sources of Silica and Surfactant:

S.no	Surfactant	Silica Sources
1.	Tetraethyl Orthosilicate	Cetyltrimethylammonium Bromide
2.	Sodium Silicate	Tween 80
3.	Silica Dioxide	Span 80

2.2 Formulation of silymarin loaded mesoporous silica nanoparticle and folic acid coated:

Silymarin (20 mg/ml) in methanol was added to 1 g MSNs and stirred at 60 °C for 4 hours [18]. Folic acid (15 mg) was mixed in 30 ml water at 60 °C, cooled, and mixed with silymarin-loaded

MSNs. The mixture was stirred for 4 hours, stored overnight, then at 4000 rpm centrifugation happen for 20 minutes to obtain stable folic acid-coated MSNs.

2.3 Optimization of MSNs:

The optimization of MSNs was carried out using a Box-Behnken design (BBD) with Design Expert 13 software, involving three factors TEOS amount (X1), CTAB (X2), and 2M NaOH (X3) and three responses: particle size (Y1), PDI (Y2), and zeta potential (Y3). Seventeen experimental runs were designed within defined factor ranges to achieve minimal particle size, low PDI, and highly negative zeta potential. The data were fitted to linear, quadratic, or tertiary models, and analyzed using ANOVA, considering p-values, R^2, and adequate precision to validate model reliability. The optimized formulation was synthesized based on statistical predictions, revealing the interplay between synthesis variables and MSN properties [19].

Table 2 Optimization of MSNs Factors and responses used in response surface design

Response Surface Methodology design		
Independent variables		
Factors	**Low limit**	**High limit**
X1- TEOS (ml)	1	5
X2- CTAB (mg)	10	50
X3- 2M NaOH (ml)	1	10
Dependent Variables		
Response	**Goal**	
Y1- Particle size in nm	Minimise	
Y2- PDI	Minimise	
Y3- Zeta potential in mV	Most negative	

2.4 Determination of Zeta Potential and Particle Size:

Zeta potential and Particle size were analysed using a Malvern Nano-Zetasizer (Nano ZS90). Samples get diluted with deionized water for size analysis and measured at 90°; zeta potential was recorded at 25 °C using a zeta dip cell.

2.5 X ray diffraction study (XRD):

The crystal nature of mesoporous silica nanoparticles was determined using X-ray diffraction analysis. Measurements was conducted with Cu K Alpha radiation (N=1.5418A). Bruker D8 Advanced X-ray diffractometer utilizing at 40kV voltage, current at 30mA. Samples were scanned in the range of 0°-80° (20) at an increment angle of 0.02° and a counting rate of 0.3s/step.

2.6 Fourier Transform Infrared Spectroscopy (FTIR):

Samples combined with KBr, grind onto plate, and analyzed in spectrum range of 400 to 4000 cm^{-1} IN FT-IR 8400, Shimadzu 240V, Japan.

2.7 Atomic Force Microscopy (AFM):

The pure MSNs and silymarin-loaded folic acid-coated MSNs surface morphology was analyzed using AFM. Samples kept on the AFM stage, calibrated, and scanned to measure surface topography and collect morphological data.

2.8 Scanning electron microscopy (SEM):

Pure MSNs and FA-Silymarin-MSNs surface morphology was examined using SEM. Samples fixed on carbon-coated stubs, sputter-coated with osmium tetroxide, and imaged under high vacuum. MSNs showed spherical shapes, while FA-Silymarin-MSNs exhibited increased roughness and slight aggregation, confirming drug loading and coating.

2.9 *In Vitro* release of drug:

In vitro release of Pure-silymarin along with FA-Silymarin-MSNs was assessed via the dialysis bag diffusion method in (pH 7.4) phosphate buffer at 37 ± 0.5 °C. Samples collected at specific range (1,2,3,4,5,6,7,8,24 hours) and analyzed using UV–Visible spectrophotometry at 287 nm. Sink conditions were maintained by replacing the medium after each withdrawal [20].

2.10 *In Vitro* Hepatocarcinoma cell line study:

The HepG2 cells were grown in a normal incubator at 37°C with 5% CO_2, in a medium that included 10% FBS and 1% penicillin-streptomycin. We treated cells seeded in 96-well plates with different doses of free silymarin. and FA-Silymarin-MSNs for 24 hours in order to determine their cytotoxicity. The cell density was 5×10^3 cells/well. MTT assay was performed, and absorbance was measured at 570 nm to determine cell viability and calculate IC_{50} values for comparative analysis [21].

3. RESULT:

3.1 Screening of Mesoporous Silica Nanoparticle:

The best combination for preparing mesoporous silica nanoparticles is Tetraethyl Orthosilicate with Cetyltrimethylammonium Bromide**.** This combination achieved the smallest particle size (531.9 nm) with the highest stability, as indicated by the strongly negative zeta potential (−45.6 mV) and the lowest PDI (0.104).

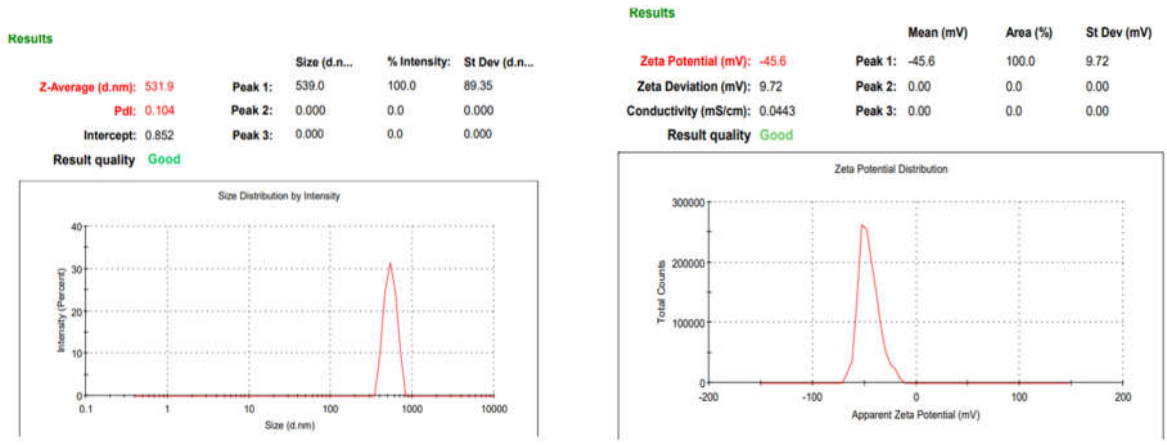

A) **B)**

Figure.1 A) Particle size and B) Zeta potential for Screening of Mesoporous Silica Nanoparticles in TEOS and CTAB Combination

3.2 MSNs Optimization:

The optimized mesoporous silica nanoparticles developed using the Box–Behnken design exhibited uniform particle size, narrow size distribution, and stable surface charge. The formulation parameters were successfully adjusted to achieve desirable physical characteristics, ensuring consistent morphology and colloidal stability suitable for drug delivery applications. Result Shown in Table 2,3,4,5,6.

Table 3 Experiments configuration and observation response design:

Run	Factors			Response		
	X1	X2	X3	Y1	Y2	Y3
	TEOS (ml)	CTAB (mg)	2M NaOH (ml)	Particle size (nm)	PDI	Zeta potential (mV)
1	3	10	10	869.9	0.856	-42.5
2	3	30	5.5	533.6	0.216	-56.9
3	3	10	1	608	0.290	-59.2
4	1	50	5.5	496	0.782	-30.9
5	3	30	5.5	456	0.209	-45.1
6	3	50	1	488	0.981	-49.6
7	3	30	5.5	439	0.241	-51.8
8	3	30	5.5	404.6	0.024	-51.5
9	5	10	5.5	568	0.524	-63.8
10	5	50	5.5	1056	1	-25.1
11	1	10	5.5	482.1	0.670	-63.5
12	5	30	1	634	0.349	-48.1
13	3	30	5.5	412	0.211	-42.1
14	1	30	1	432	0.654	-46.7

15	1	30	10	966	0.565	-38.4
16	3	50	10	1397	1	-30.5
17	5	30	10	1069	1	-39.5

Table 4 Summary of statistical analysis and model fitting:

Response	Model Suggested	F-value	P-value	R^2	R^2 Adjusted	R^2 Predicted	Adequate Precision
Y1	Quadratic	33.65	0.0500	0.9774	0.9484	0.7492	19.849
Y2	Quadratic	34.69	0.0500	0.9780	0.9498	0.9001	14.935
Y3	Linear	10.25	0.0500	0.7028	0.6342	0.4692	11.013

Table 5 Responses Coefficient equations:

Responses	Coefficient Equations
Y1	449.04+118.86A+113.63B+267.49C+118.53AB−24.75AC+161.78BC+68.01A 2 + 133.48B 2 +258.21C 2
Y2	0.1802+0.02525A+0.17788B+0.14338C+0.091AB+0.185AC−0.13675BC+0.2 1203A 2 +0.35178B 2 +0.24978C 2
Y3	−46.1882+0.375A+11.6125B+6.5875C

Table 6 optimized actual values and predicted of MSNs with (n=3, SD):

Optimized factor	Responses	Predicted Value 95%CI Low	Predicted Value	Predicted Value 95% CI High	Actual Value	Error Percentage (%)
X1:2.85	Y1	378.2	499.9	519.8	320	35.96%
X2:32.11	Y2	0.100	0.200	0.259	0.247	23.5%
X3:5.44	Y3	-49.75	-45.06	-42.61	-47.6	5.63%

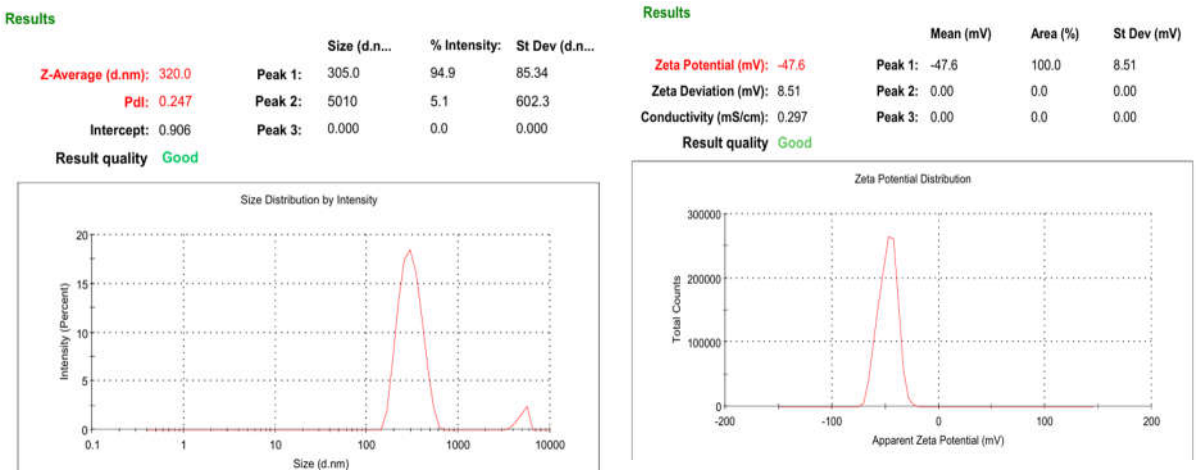

A) **B)**

Figure.2 A) size of particle and B) Zeta potential for Optimization of MSNs

The optimization study showed a high desirability value of 0.967, confirming effective optimization of particle size (449.997 nm), PDI (0.200001), and zeta potential (-45.0693 mV). TEOS and CTAB had a simultaneous effect on particle growth, while moderate concentrations minimized PDI and enhanced stability. Contour and 3D plots validated the model's reliability for developing stable, uniform MSNs for drug delivery. Result shown in Fig 3,4,5,6.

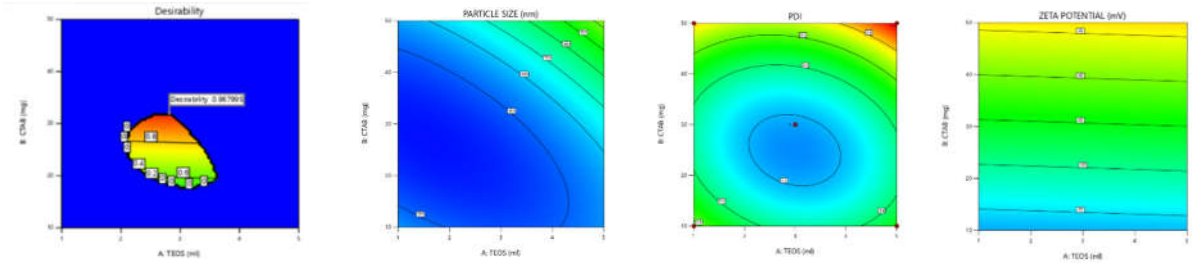

A) **B)** **C)** **D)**

Figure.3 Contour plots A) Desirability, B) Particle Size, C) PDI, D) Zeta Potential

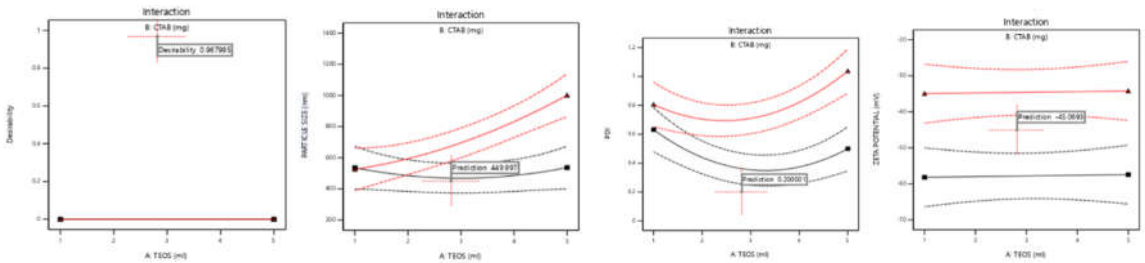

A) **B)** **C)** **D)**

Figure.4 Interaction plots A) Desirability, B) Particle Size, C) PDI, D) Zeta Potential

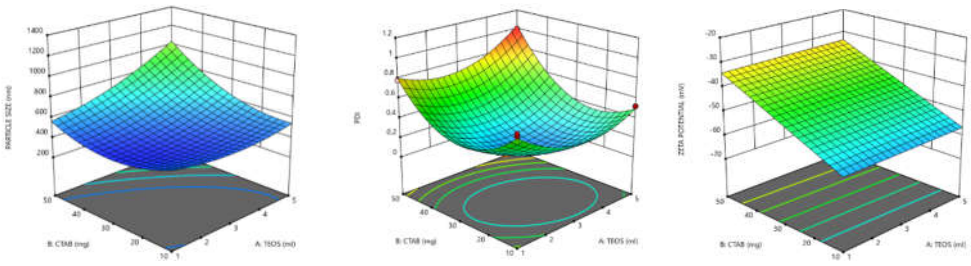

A) **B)** **C)**

Figure.5 Three-dimensional surface plots. (A), Y1: particle size;(B) Y2: PDI;(C), Y3: zeta potential.

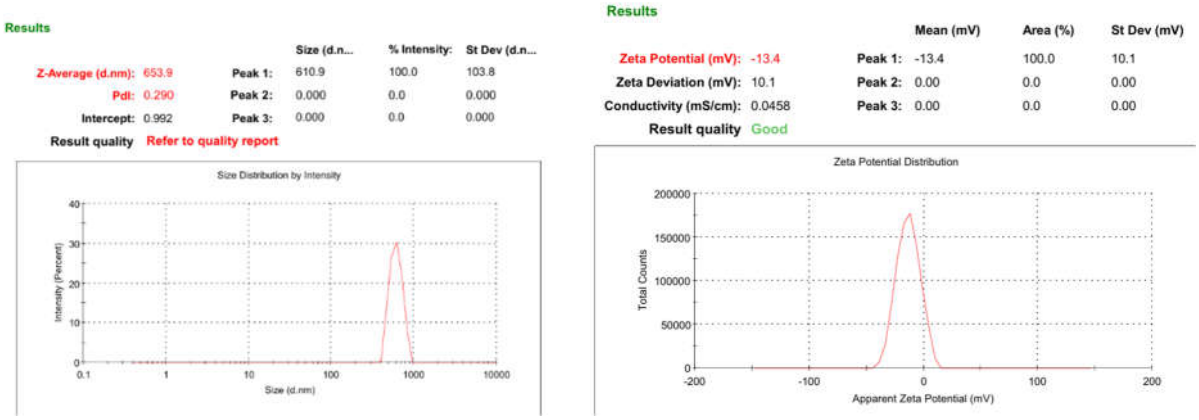

A) **B)**

Figure.6 A) size of particle and B) Zeta potential silymarin loaded mesoporous silica nanoparticle and folic acid coated

3.3 XRD:

The XRD diffraction of pure silymarin showed sharp peaks, indicating its crystalline nature, while the silymarin-loaded folic acid-coated MSNs showed a broad hump at 20°–30° 2θ, confirming an amorphous form. [20] Result shown in Fig.7

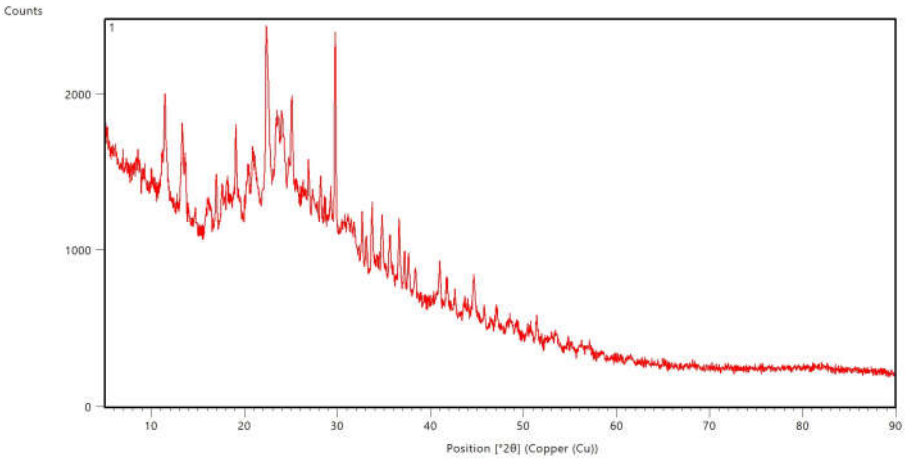

A)

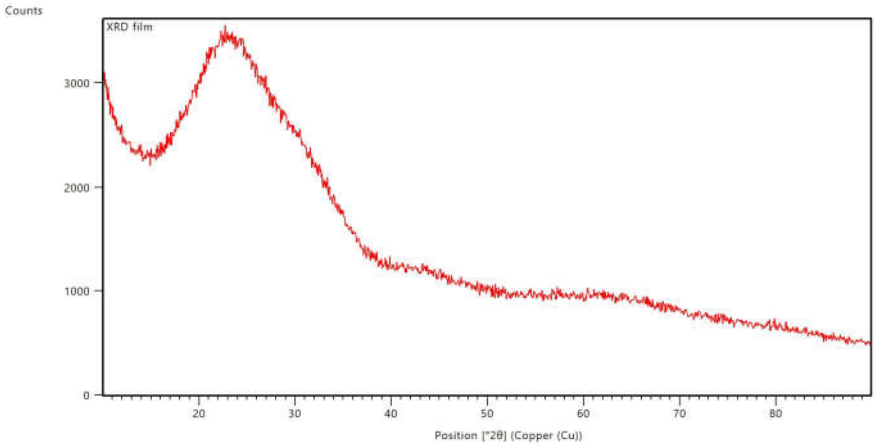

B)

Figure.7 XRD A) Silymarin B) Silymarin loaded folic acid coated MSNs

3.4 FTIR:

FTIR spectrum confirmed successful silymarin incorporation by retaining O–H and C=O peaks, along with Si–O–Si and Si–O–C bands indicating silica framework formation. C–H peaks showed CTAB presence, while folic acid peaks confirmed surface functionalization. A broad O–H band suggested hydrogen bonding, enhancing drug stability and encapsulation. [22] Result shown in Fig.8

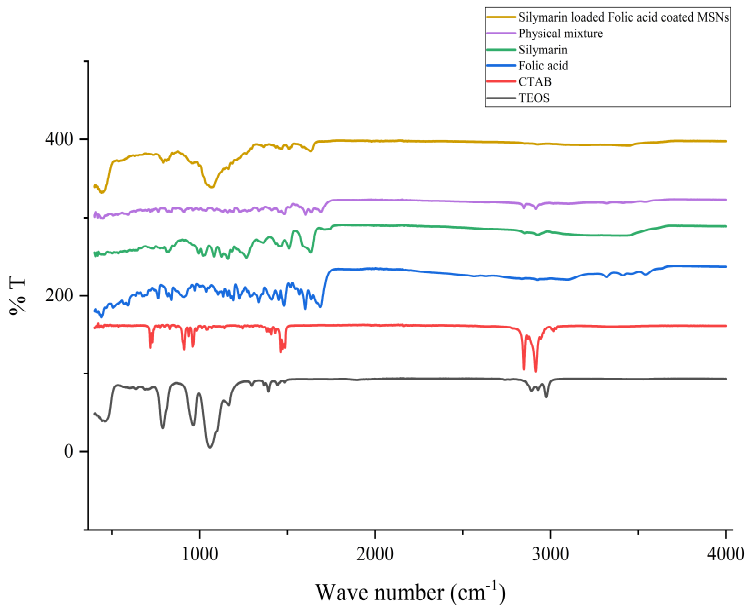

Figure.8 FTIR Spectrum of TEOS, CTAB, Folic acid, Silymarin, Physical mixture, Silymarin loaded Folic acid Coated MSNs

3.5 AFM:

AFM finding shows a reduction in surface roughness from 452.62 nm to 90.93 nm and particle size from 2118.64 nm to 390.82 nm after silymarin loading and folic acid coating. [23] Result shown in Fig.9,10.

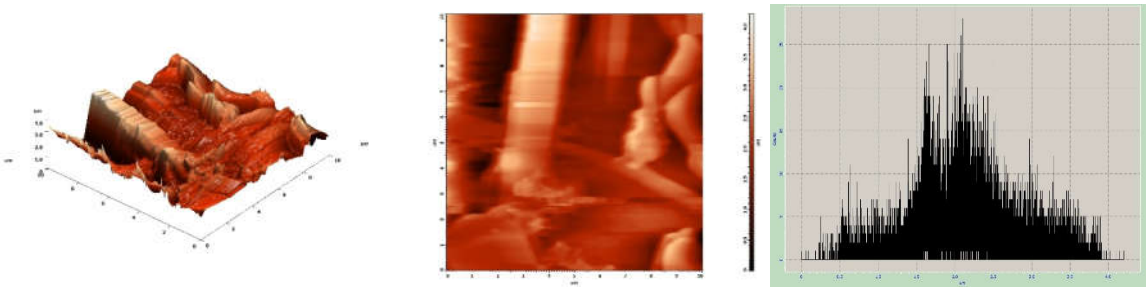

A) **B)** **C)**

Figure.9 AFM Pure Mesoporous Silica Nanoparticles; A) 3D, B) 2D, C) Histogram

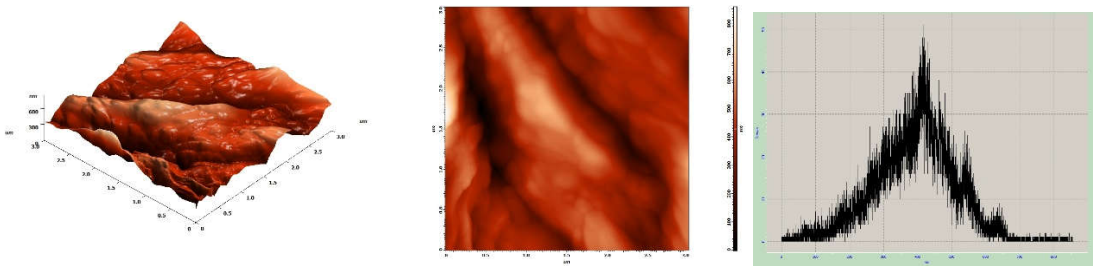

A) **B)** **C)**

Figure.10 AFM Silymarin loaded Folic Acid Coated Mesoporous Silica Nanoparticles; A) 3D, B) 2D, C) Histogram

3.6 SEM:

The scanning electron microscopy (SEM) images revealed that the synthesized mesoporous silica nanoparticles (MSNs) exhibited a uniform, spherical morphology with a smooth surface and well-defined particle boundaries, indicating successful synthesis. Upon loading with silymarin and coating with folic acid, the particles maintained their spherical structure, with a slightly roughened surface texture, confirming surface functionalization. The particle size distribution appeared consistent, with no significant aggregation observed, suggesting excellent stability. These results demonstrate the successful fabrication of silymarin-loaded,

folic acid-coated MSNs with desirable structural integrity for targeted drug delivery applications. Result shown in Fig.11,12.

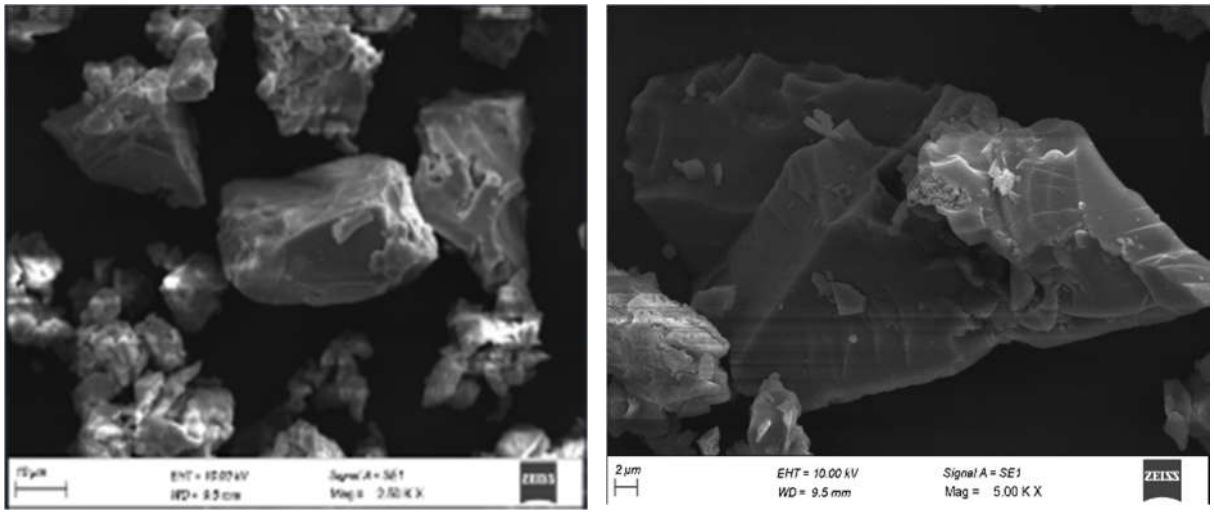

A) **B)**

Figure.11 Silymarin loaded folic acid coated MSNs a)10µm b) 2µm

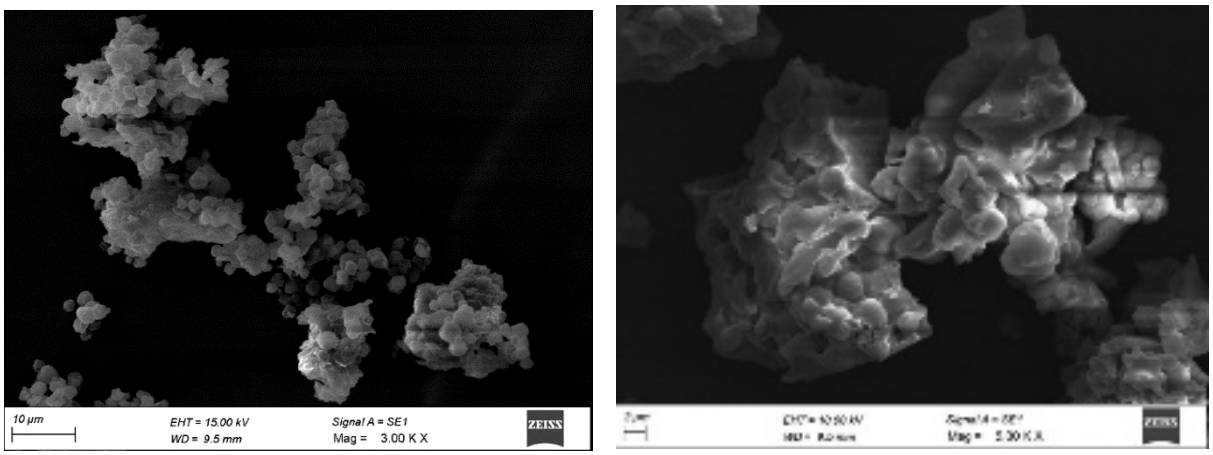

A) **B)**

Figure.12 Mesoporous Silica Nanoparticles A) 10µm B) 2µm

3.7 *In Vitro* drug release:

The optimized folic acid-coated MSNs showed a cumulative drug release of 67.9% after 24 hours, compared to 39.4% for pure silymarin. Result shown in Table 7 and Fig.13.

Table 7 Percentage of *In-Vitro* drug release profile of Silymarin and Optimized Silymarin Loaded Folic Acid Coated MSNs:

Time(hours)	% of drug release	
	Silymarin	Optimized Silymarin Loaded Folic Acid Coated MSNs
1	5.2	11.5
2	9	19
3	15.1	24.6
4	19.3	30.1
5	23.4	39
6	27.8	42.5
7	30	51.2
8	34.2	55
24	39.4	67.9

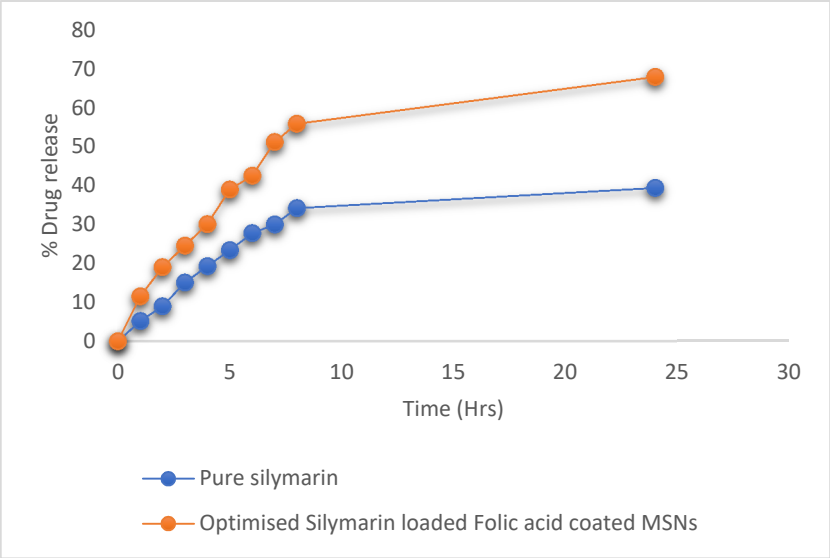

Figure.13 *In Vitro* drug release of Pure Silymarin and Optimised Silymarin loaded Folic acid Coated MSNs

3.8 *In-Vitro* hepatic cell line study:

Cytotoxicity studies showed free silymarin had an IC_{50} of 39.877 µg/ml, indicating moderate potency. Silymarin-loaded folic acid-coated MSNs had a higher IC_{50} of 55.750 µg/ml, reflecting sustained release, reduced initial toxicity, and improved biocompatibility. Result shown in Table 8,9. Result shown in Fig.14,15,16.

Table 8 Result of free drug Silymarin anticancer activity with IC50:

Concentration µg/ml	Free drug-Silymarin		
	Cell Viability (%)	Cytotoxicity (%)	IC50 Value
0.78	95.92	4.08	39.877
1.56	92.47	7.53	
3.125	83.90	16.10	
6.25	72.55	27.45	
12.5	60.15	39.85	
25	46.40	53.60	
50	34.19	65.81	
100	21.84	78.16	

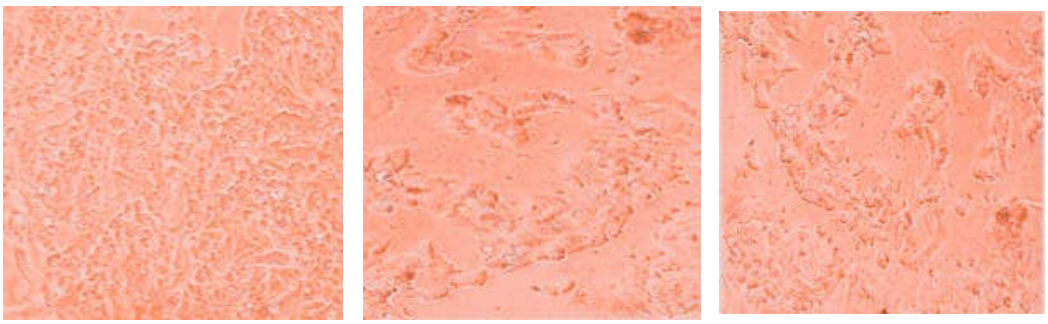

A) **B)** **C)**

Figure.14 Result of free drug Silymarin anticancer activity A) Control, B) 50µg/ml, C) 100µg/ml

Table 9 Result of Silymarin loaded folic acid coated MSNs anticancer activity with IC50:

Concentration µg/ml	Silymarin loaded folic acid coated MSNs		
	Cell Viability (%)	Cytotoxicity (%)	IC50 Value
0.78	98.35	1.65	55.750
1.56	95.66	4.34	
3.125	92.81	7.19	
6.25	85.99	14.01	
12.5	75.92	24.08	
25	66.55	33.45	
50	43.71	56.29	
100	30.34	69.66	

A) **B)** **C)**

Figure.15 Result of Silymarin loaded folic acid coated MSNs anticancer activity A) Control, B) 50µg/ml, C) 100µg/ml

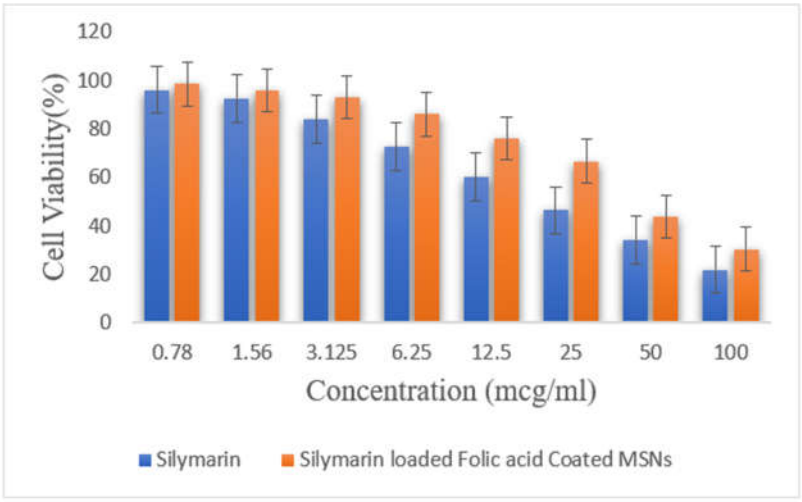

Figure.16 HepG2 Cell line Silymarin and Silymarin loaded Folic acid Coated MSNs

4. DISCUSSION:

The observed increase in particle size can be attributed to the catalytic role of sodium hydroxide during the sol–gel process. At higher concentrations, NaOH rapidly hydrolyzes TEOS, generating a large number of silanol groups that undergo condensation in a short time frame. This accelerated reaction favors particle growth over nucleation, leading to the formation of larger silica frameworks rather than small, discrete nanoparticles. The interactive effect between NaOH and TEOS further enhances this phenomenon by promoting extensive cross-linking, which contributes to bulkier structures. In addition, CTAB concentration played a complementary role in particle growth. While moderate amounts of CTAB stabilize the micelles and maintain uniform particle formation, excessive levels result in micelle aggregation and disordered pore expansion, which further enlarges particle size. These combined effects explain why higher NaOH levels, particularly in the presence of increased TEOS and CTAB,

shift the balance from controlled nucleation toward uncontrolled growth, resulting in significantly larger nanoparticles. Statistical validation through ANOVA confirmed the model's reliability, with no lack of fit, while diagnostic plots further supported its accuracy. The optimized conditions predicted particles of ≈378 nm with a PDI of 0.20 and a zeta potential of –49.7 mV, which aligned closely with experimental findings (320 nm, 0.247, –47.6 mV). Subsequent folic acid coating improved surface smoothness, enhanced dispersion stability, and provided favorable conditions for effective drug–nanocarrier interactions.

FTIR spectra validated the presence of Si–O–Si and Si–O–C frameworks, with additional bands confirming successful incorporation of silymarin and folic acid functionalization. A broad O–H absorption band suggested hydrogen bonding, which maintained silymarin in an amorphous state. This was further supported by XRD data, which showed the disappearance of sharp crystalline peaks and the appearance of a broad halo, characteristic of amorphous dispersion. AFM analysis revealed a sharp decline in surface roughness, decreasing from 452.6 nm to 90.9 nm after drug loading and coating, while SEM images displayed spherical particles with slightly irregular surfaces, consistent with successful functionalization. Collectively, these characterizations confirmed stable encapsulation of silymarin within FA-MSNs.

FA-MSNs achieved a substantially higher 24-hour cumulative release (67.9% vs 39.4% for free silymarin), showing that the mesoporous silica framework plus folic acid functionalization promotes sustained, higher drug availability over 24 hours. The SLN system showed a biphasic release (rapid surface/burst release followed by slower core release), and kinetics best fit the Higuchi model (R^2 = 0.9948), indicating a diffusion-controlled release mechanism from the lipid matrix. Mechanistically, FA-MSNs deliver faster cumulative release because the drug is held in amorphous form within open mesopores and stabilized by hydrogen bonding (FTIR/XRD/AFM data), whereas SLNs trap the drug within a solid lipid core (high EE ~81%) that slows desorption but limits recrystallization. Functionally, the two platforms differ: FA-MSNs favor higher soluble drug exposure and receptor-mediated uptake for tumor targeting, while SLNs produce superior barrier permeation and a depot-like, prolonged release (SLN ex vivo permeation exceeded suspension—e.g., ≈71.2% vs 42.2% at 8 h). [22]

The HepG2 cell line comparison between the two studies reveals distinct cytotoxic and mechanistic behaviors of silymarin delivery. In the study, free silibinin exhibited a rapid, dose-dependent cytotoxic effect on HepG2 cells, with cell viability decreasing sharply even at moderate concentrations due to direct apoptotic induction, as confirmed by acridine orange/PI staining and Lactate Dehydrogenase (LDH) leakage. However, in the FA-MSN study, silymarin-loaded folic acid-functionalized mesoporous silica nanoparticles displayed a more gradual cytotoxic profile, with a higher IC_{50} (55.75 µg/mL) compared to free silymarin (39.88 µg/mL), suggesting reduced initial toxicity and controlled intracellular release. Morphologically, HepG2 cells treated with FA-MSNs exhibited gradual apoptosis through folate receptor-mediated uptake, unlike the direct necrotic–apoptotic transition observed in free drug exposure. Thus, while silibinin acts as a potent cytotoxic agent causing immediate apoptosis, FA-MSNs offer prolonged, targeted, and safer anti-hepatocarcinoma activity through sustained drug delivery and receptor-specific internalization. [24]

5. CONCLUSION:

The Box–Behnken optimized FA-MSNs demonstrated uniform particle size, enhanced colloidal stability, high encapsulation efficiency, and receptor-mediated targeting ability. This formulation effectively overcame the limitations of silymarin's poor solubility and instability while enabling controlled release and selective tumor delivery, establishing it as a more advanced alternative to conventional systems.

ABBREVIATIONS:

SL	Silymarin
FA	Folic acid
MSNs	Mesoporous silica nanoparticles
HCC	Hepatocellular carcinoma
FOLR1	Folate Receptor 1
FTIR	Fourier-transform infrared spectroscopy
XRD	X-ray diffraction
SEM	Scanning electron microscopy
AFM	Atomic force microscopy
CTAB	Cetyltrimethylammonium bromide
TEOS	Tetraethyl orthosilicate
BBD	Box Behnken design
pH	Potential of Hydrogen
µg	Microgram
g	Gram
ml	Milliliter
mg	Milligram
IC	Inhibitory Concentration
HepG2	Human liver cancer cell
PDI	Poly dispersity index
UV	Ultra violet

ACKNOWLEDGMENTS:

The authors thank the Department of Pharmaceutics, PSG College of Pharmacy, Coimbatore, for their help in using resources and facilities for this study, and The Tamil Nadu Dr. M.G.R Medical University, Chennai, for academic guidance and affiliation.

FINANCIAL SUPPORT:

No

CONFLICTS OF INTEREST:

No

REFERENCES:

1) Ghalehkhondabi V, Soleymani M, Fazlali A. Folate-targeted nanomicelles containing silibinin as an active drug delivery system for liver cancer therapy. Journal of Drug Delivery Science and Technology. 2021 Feb;61:102157.
2) Garg S, Peeters M, Mahajan RK, Singla P. Loading of hydrophobic drug silymarin in pluronic and reverse pluronic mixed micelles. Journal of Drug Delivery Science and Technology. 2022 Aug 13;75:103699–9.
3) Ganne-Carrié N, Nahon P. Differences between hepatocellular carcinoma caused by alcohol and other aetiologies. Journal of Hepatology. 2024 Dec; https://doi.org/10.1016/j.jhep.2024.12.030
4) Arab JP, Díaz LA, Rehm J, Im G, Arrese M, Kamath PS, et al. Metabolic Dysfunction and Alcohol-related Liver Disease (MetALD): Position statement by an expert panel on alcohol-related liver disease. Journal of Hepatology [Internet]. 2024 Nov 1; Available from: https://www.journal-of-hepatology.eu/article/S0168-8278(24)02728-4/fulltext.
5) Devshree Dhande, Archana Dhok, Ashish Anjankar, Shailesh Nagpure. Silymarin as an Antioxidant Therapy in Chronic Liver Diseases: A Comprehensive Review. Cureus [Internet]. 2024 Aug 17 [cited 2025 Feb 8]; Available from: https://pmc.ncbi.nlm.nih.gov/articles/PMC11404857/.
6) Ranjan S, Gautam A. Pharmaceutical prospects of Silymarin for the treatment of neurological patients: an updated insight. Frontiers in Neuroscience. 2023 May 18;17.
7) Seo S, Kim GY, Kim MH, Lee KW, Kim MJ, Chaudhary M, et al. Nanocrystal Formulation to Enhance Oral Absorption of Silybin: Preparation, In Vitro Evaluations, and Pharmacokinetic Evaluations in Rats and Healthy Human Subjects. Pharmaceutics. 2024 Aug 2;16(8):1033–3.
8) Lérida-Viso A, Estepa-Fernández A, García-Fernández A, Martí-Centelles V, Martínez-Máñez R. Biosafety of mesoporous silica nanoparticles; towards clinical translation. Advanced Drug Delivery Reviews [Internet]. 2023 Oct 1;201:115049. Availablfrom: https://www.sciencedirect.com/science/article/pii/S0169409X23003642#b0035.
9) Liu B, Liu W, Xu M, Zhao T, Zhou B, Zhou R, et al. Drug delivery systems based on mesoporous silica nanoparticles for the management of hepatic diseases. Acta Pharmaceutica Sinica B [Internet]. 2024 Dec 20; Available from: https://www.sciencedirect.com/science/article/pii/S2211383524004726?via%3Dihub.

10) Young O, Ngo N, Lin L, Stanbery L, Creeden JF, Hamouda D, et al. Folate Receptor as a Biomarker and Therapeutic Target in Solid Tumors. Current Problems in Cancer. 2023 Feb;47(1):100917.
11) Yuto Shiode, Kodama T, Sato Y, Takahashi R, Takayuki Matsumae, Shirai K, et al. Folate receptor 1 is a stemness trait-associated diagnostic and prognostic marker for hepatocellular carcinoma. Biomarker Research. 2025 Mar 4;13(1).
12) Ren B, Chen DF, Zhao XJ, Li LS, Zhao MX. Evaluating biological activity of folic acid-modified and 10-hydroxycamptothecin-loaded mesoporous silica nanoparticles. Materials Chemistry and Physics. 2022 Dec;292:126756.
13) Dominik Šafčák, Dražilová S, Gazda J, Igor Andrašina, Adamcová-Selčanová S, Barila R, et al. Alcoholic Liver Disease-Related Hepatocellular Carcinoma: Characteristics and Comparison to General Slovak Hepatocellular Cancer Population. Current Oncology [Internet]. 2023 Mar 22 [cited 2024 Feb 10];30(3):3557–70. Available from: https://www.ncbi.nlm.nih.gov/pmc/articles/PMC10047624/.
14) Nikolett Szpisják-Gulyás, Al-Tayawi AN, Z. Horváth, Zs. László, Szabolcs Kertész, Cecília Hodúr. Methods for experimental design, central composite design and the Box–Behnken design, to optimise operational parameters: A review. Acta Alimentaria. 2023 Dec 4;52(4):521–37.
15) Santhy WYANTUTI, Balqis FADHILATUNNISA, Retna Putri FAUZIA, JIA Q, RAHMANI AA, None IRKHAM, et al. Response surface methodology box-behnken design to optimise the hydrothermal synthesis of gadolinium nanoparticles. CHINESE JOURNAL OF ANALYTICAL CHEMISTRY (CHINESE VERSION). 2023 Sep 26;51(10):100316–6.
16) Yang L, Zheng P, Chen Z. Optimization of the preparation of chitosan nanoparticles loaded with bifendate using the box–Behnken design. Results in Chemistry. 2025 Feb 1;102085–5.
17) Fatima R, Katiyar P, Kushwaha K. Recent advances in mesoporous silica nanoparticle: synthesis, drug loading, release mechanisms, and diverse applications. Frontiers in Nanotechnology. 2025 Mar 18;7.
18) Selc M, Radka Macova, Babelova A. Nanoparticle-boosted silymarin: Are we overlooking taxifolin and other key components? Frontiers in Plant Science. 2025 Aug 15;16.
19) Kim M, Ki DH, Young-Guk Na, Hae Young Lee, Baek JS, Jae Sung Lee, et al. Optimization of Mesoporous Silica Nanoparticles through Statistical Design of Experiment and the Application for the Anticancer Drug. 2021 Jan 31;13(2):184–4.
20) Shriram RG, Moin A, Alotaibi HF, Khafagy ES, Al Saqr A, Abu Lila AS, et al. Phytosomes as a Plausible Nano-Delivery System for Enhanced Oral Bioavailability and Improved Hepatoprotective Activity of Silymarin. Pharmaceuticals. 2022 Jun 24;15(7):790. https://doi.org/10.3390/ph15070790.
21) Wang H, Shen X, Zhu X, Zeng S, Cai S. Enhancing HepG2 cell apoptosis with a combined nanoparticle delivery of miR-128-3p agomir and Oroxin B: A novel drug delivery approach based on PI3K-AKT and VEGF pathway crosstalk. Asian Journal of

PharmaceuticalSciences.2024Apr1;100909–9.
https://doi.org/10.1016/j.ajps.2024.100909

22) Poonam Kumari. Development, Characterization and Validation of Silymarin Loaded Solid Lipid Nanoparticles for the Treatment of Liver Cirrhosis. Journal of Pharmaceutical Negative Results. 2022;13(7):7.
23) Pergal MV, Jelena Brkljačić, Gordana Tovilović-Kovačević, Milena Špírková, Kodranov ID, Manojlović DD, et al. Effect of mesoporous silica nanoparticles on the properties of polyurethane network composites. Progress in Organic Coatings. 2020 Dec 3;151:106049–9.
24) Niki Vakili Zahir. Evaluation of Silibinin Effects on the Viability of HepG2 (Human hepatocellular liver carcinoma) and HUVEC (Human Umbilical Vein Endothelial) Cell Lines. Iranian Journal of Pharmaceutical Research. 2018.